

Synthesis, structure, lattice energy and enthalpy of 2D hybrid perovskite $[\text{NH}_3(\text{CH}_2)_4\text{NH}_3]\text{CoCl}_4$, compared to $[\text{NH}_3(\text{CH}_2)_n\text{NH}_3]\text{CoCl}_4$, $n=3-9$

Seham K. Abdel-Aal*, Ahmed S. Abdel-Rahman

Physics Department, Faculty of Science, Cairo University, 12613, Egypt

ARTICLE INFO

Communicated by: Andrea Zappettini

Keywords:

- A1. Crystal structure
- A2. Growth from high temperature solutions
- A2. Single crystal growth
- A3. Quantum wells
- B1. Perovskites
- B1. Inorganic compound

ABSTRACT

A new organic-inorganic 2D hybrid perovskite $[\text{NH}_3(\text{CH}_2)_4\text{NH}_3]\text{CoCl}_4$, 1,4butane diammonium tetrachlorocobaltate, has been synthesized. Blue prismatic single crystals were grown from ethanolic solution in 1:1 stoichiometric ratio (organic/inorganic) by gradual cooling to room temperature after heating at 70 °C for 1 h. The hybrid crystallizes in a triclinic phase with the centrosymmetric space group $\bar{P}\bar{1}$. Its unit cell parameters are $a=7.2869(2)$ Å, $b=8.1506(2)$ Å, $c=10.4127(3)$ Å, $\alpha=77.2950(12)^\circ$, $\beta=80.0588(11)^\circ$, $\gamma=82.8373(12)^\circ$ and $Z=2$. The final R factor is 0.064. The structure consists of organic cations $[\text{NH}_3(\text{CH}_2)_4\text{NH}_3]^{2+}$ which act as spacer between layers of inorganic dianions $[\text{CoCl}_4]^{2-}$ in which Co²⁺ ions are coordinated by four Cl atoms in an isolated tetrahedral structure. The organic and inorganic layers form infinite 2D sheets which are parallel to the ac plane, stacking alternatively along the b -axis, and are connected via N-H...Cl hydrogen bonds. The lamellar structure of the 1,4 butane diammonium tetrachlorocobaltate hybrid is typically considered as naturally self-assembled multiple quantum wells (MQW). The calculated lattice potential energy U_{pot} (kJ/mol) and lattice enthalpy ΔH_L (kJ/mol) are inversely proportional to the molecular volume V_m (nm³) of perovskite hybrid of the formula $[\text{NH}_3(\text{CH}_2)_n\text{NH}_3]\text{CoCl}_4$, $n=3-9$.

© 2016 Elsevier B.V. All rights reserved.

1. Introduction

Compounds with the general formula A_2MX_4 (A =organic cation, M =divalent metal ion and $X=Cl^-$, Br^- , I^-) are known to be crystallized in 2D perovskite-like structure and are usually referred to as organic-inorganic hybrid perovskites (OIHSs) or organo-metal halide composite [1–3]. OIHSs attract much attention in the last 2 decades as they combine both the organic and inorganic characteristics in a single molecular-scale nanocomposite. Unique structure, electrical, magnetic, optical, excitonic, electronic and optoelectronic properties in this class of materials have been widely reported in literature [3–17].

In the hybrid perovskites A_2MX_4 , if A is an ammonium substituted organic cation, $R-\text{NH}_3$ (R =organic cation), it is usually called monoammonium (bilayer) where the NH_3 group is attached to the end of the organic chain. The general formula can be written as $(R-\text{NH}_3)_2\text{MX}_4$, and the reaction stoichiometric ratio of organic and inorganic part is (2:1) [4]. For diammonium hybrid perovskite (monolayer) of a formula $(\text{NH}_3-R-\text{NH}_3)\text{MX}_4$, in which NH_3 group is

attached to both ends of the organic chain [1,2,13,16,17], the reaction stoichiometric organic/inorganic ratio is (1:1). Basically, the structure of 2D hybrid perovskites consists of organic cation layers and metal halide layers, which are stacking alternatively. The ammonium ions at both ends of the organic chain form $[\text{N}-\text{H} \dots \text{X}]$ hydrogen bonds with the halide ions of the inorganic layers which stabilize the layered structure and make these materials good candidates as proton conductors [15,17], also with potential application for UV detection [13]. The alternative structure, low dimensionality and difference in the dielectric properties of organic/inorganic layers make these hybrid perovskites to possess Mott type excitons that have been observed even at room temperature [7–14]. OIHSs are naturally self organized multiple quantum wells. The wells are made of metal halide (inorganic) sheets clad by barriers of (organic) layers [10,11,14].

The physical and chemical properties of OIHSs depend on (1) characteristics of the organic cations (aliphatic, aromatic, chain length, functional attached group); (2) inorganic anion coordination geometry of the metal ion, $[\text{MX}_4]^{2-}$ or $[\text{MX}_6]^{2-}$, (M =transition metals, Alkali earth metals, Alkali metals, other metals), (3) halogen Cl^- , Br^- , I^- , and (4) reaction stoichiometric ratio (organic/inorganic), which allows the properties of hybrid

* Corresponding author.

E-mail address: seham@sci.cu.edu.eg (S.K. Abdel-Aal).

perovskites to be tailored [1–10]. It is clear that the properties of OIHs are functions of R, M and X, and it is of great importance to investigate the structure directing properties of these new materials [1,2,5,6,16,17].

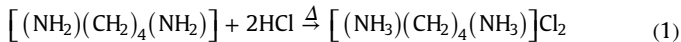
The hybrid perovskite of diammonium series $[\text{NH}_3\text{-(CH}_2\text{n-NH}_3\text{)}\text{MX}_4]$ ($n=2, 3, 4, \dots$, $\text{X}=\text{Cl}$, $\text{M}=\text{divalent metal ions}$), has been intensively investigated in the last two decades, due to their interesting physical, chemical properties and data storage applications, besides the existence of numerous structural phase transitions. For $\text{M}=\text{Mn}$ [18,19], Pb [20,21], Sn [22], Cd [15,19,23], Cu [24–26], Pd [26], structure forms corner shared octahedron $[\text{MX}_6]^{2-}$ alternated with organic layers. While for $\text{M}=\text{Co}$ [16,17,27–29], Zn [13,30,31] isolated tetrahedral structures are formed for the inorganic layer $[\text{MX}_4]^{2-}$ sandwiched between layers of organic cation.

It is to know the lattice potential energy U_{pot} (kJ/mol) and lattice enthalpy ΔH_L (kJ/mol) in order to understand the stability of new materials [32–34] especially the materials with potential technological applications [1,6,8,11]. There has been no result reported for hybrid perovskites with lower thickness of organic layer $n=4$, $\text{M}=\text{Co}^{II}$, $\text{X}=\text{Cl}$. It is of interest to prepare single crystal and to study the room temperature crystal structure of 2D perovskite hybrid $[\text{NH}_3(\text{CH}_2)_4\text{NH}_3]\text{CoCl}_4$, 1,4 butane diammonium tetrachlorocobaltate and compare its crystal structure, lattice energy and lattice enthalpy with other related compounds having different organic chain length of diammonium series, $[\text{NH}_3(\text{CH}_2)_n\text{NH}_3]\text{CoCl}_4$, ($n=3, 5, 6, 7, 9$, $\text{M}=\text{Co}^{II}$ $\text{X}=\text{Cl}$), which have been previously published in literatures [16,17,27–29].

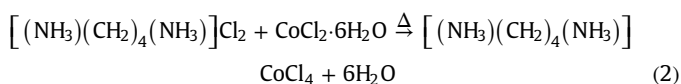
2. Experimental

2.1. Synthesis

All chemicals were purchased from SIGMA-ALDRECH and used as received. The purity of the products used is exceeding 99%. Solvents were of reagent grade. The organic salt $[\text{NH}_3(\text{CH}_2)_4\text{NH}_3]\text{Cl}_2$ were synthesized by adding drops of 30% HCl to 5 g 1,4-diaminobutane dissolved in 200 ml ethanol and placed in an ice bath till pH reaches ~4. The resulting solution is heated to 70 °C for 1 h under constant stirring. Colorless needle crystals of $[\text{NH}_3(\text{CH}_2)_4\text{NH}_3]\text{Cl}_2$ precipitate in a double wall container upon slowly cooling to room temperature. The reaction proceeds with Eq. (1).



The crystals were filtered and dried, and then kept in vacuum desiccator in N_2 gas atmosphere until use. Hybrid perovskite of $[\text{NH}_3(\text{CH}_2)_4\text{NH}_3]\text{CoCl}_4$ was prepared by mixing 1 M of ethanolic solution of both $[\text{NH}_3(\text{CH}_2)_4\text{NH}_3]\text{Cl}_2$ and of $\text{CoCl}_2 \cdot 6\text{H}_2\text{O}$ in 1:1 stoichiometric ratio, under constant stirring, which was heated to 70 °C for 1 h followed by slow cooling to room temperature in a double wall container. Blue prismatic crystals of $[\text{NH}_3(\text{CH}_2)_4\text{NH}_3]\text{CoCl}_4$ precipitate out, and the reaction proceeds with equation (2).



Blue crystallites of $[\text{NH}_3(\text{CH}_2)_4\text{NH}_3]\text{CoCl}_4$ were redissolved again and recrystallized with very slow rate of evaporation in a double wall container to obtain good untwinned and not cracked single crystals ready for single crystal X-ray investigation. The hybrid crystals were kept in a vacuum desiccator in N_2 gas atmosphere till use. Microchemical analyses were carried out to

determine the carbon, nitrogen, hydrogen concentration. It was found that the weight percentage (wt%) for C, N, H is 16.49%, 9.62%, 4.8%, respectively, very close the expected value of 16.29%, 9.39%, 4.91%, calculated from the stoichiometric formula.

2.2. IR Spectroscopy

The IR spectra between 4000–400 cm^{-1} were obtained using an FTIR 4100 spectrometer using pure KBr pellets. Chemical analysis and IR spectra confirm the formation of hybrid perovskite $[(\text{NH}_3)(\text{CH}_2)_4(\text{NH}_3)]\text{CoCl}_4$.

2.3. Crystal structure

A good crystal was selected for single crystal X-ray measurements. The single crystal X-ray crystallographic data were collected on Enraf-Nonius 590 Kappa CCD single crystal diffractometer with a graphite monochromator using Mo K α radiation ($\lambda=0.71073 \text{ \AA}$). The intensities were collected at room temperature (298 K) using $\varphi\text{-}\omega$ scan mode; the crystal to detector distance was 40 mm. The cell refinement and data reduction were carried out using Denzo and Scalepak programs [35]. The crystal structure was solved by the direct method using SIR92 program [36] which revealed the positions of all non-hydrogen atoms and refined by the full matrix least square refinement based on F^2 using maXus package [37]. Absorption corrections were applied to all data using the program SORTAV [38]. The anisotropic temperature factors of all non-hydrogen atoms were refined, and then hydrogen atoms were introduced as a riding model with C–H=0.96 \AA and refined with isotropic temperature factor. Molecular graphics were prepared using ORTEP [39], Hg and DIAMOND programs.

3. Results and discussion

3.1. IR spectroscopy

Fig. 1 shows a room temperature IR spectrum of $[(\text{NH}_3)(\text{CH}_2)_4(\text{NH}_3)]\text{CoCl}_4$. **Table 1** lists the observed absorption bands and their assignments at room temperature of $[(\text{NH}_3)(\text{CH}_2)_4(\text{NH}_3)]\text{CoCl}_4$, denoted as 2C4CoCl and other member of previously published diammonium family, such as $[(\text{NH}_3)(\text{CH}_2)_7(\text{NH}_3)]\text{CoCl}_4$, denoted as 2C7CoCl [17], $[(\text{NH}_3)(\text{CH}_2)_9(\text{NH}_3)]\text{CuCl}_4$, denoted as 2C9CuCl [40], $[(\text{NH}_3)(\text{CH}_2)_{10}(\text{NH}_3)]\text{ZnCl}_4$, denoted as 2C10ZnCl [31] and $[(\text{NH}_3)(\text{CH}_2)_{12}(\text{NH}_3)]\text{CdCl}_4$, denoted as 2C12CdCl [15] for comparison.

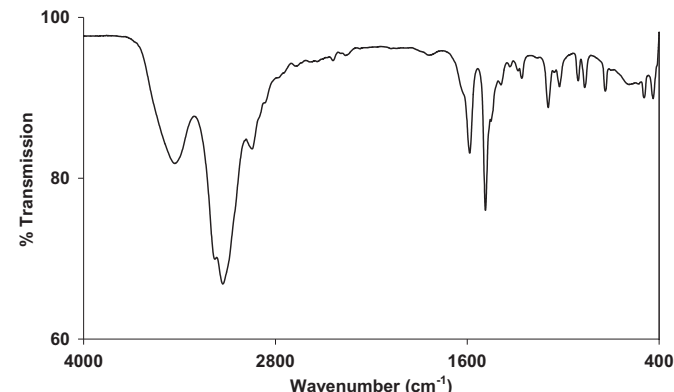


Fig. 1. IR spectrum of $[(\text{NH}_3)(\text{CH}_2)_4(\text{NH}_3)]\text{CoCl}_4$ between 4000 and 400 cm^{-1} at room temperature.

Table 1

Room temperature absorption bands and their assignment of 2C4CoCl, 2C7CoCl, 2C9CuCl, 2C10ZnCl and 2C12CdCl.

IR wave number (cm^{-1})	Attributed to				
2C4CoCl ^a	2C7CoCl [17]	2C9CuCl [40]	2C10ZnCl [31]	2C12CdCl [15]	
3446	3424	3425	3540	3631	C–H Str.
3138	3199	3125	3063	3111	C–H str/(NH ₃) ⁺ (vs.)
2957	2860	2852	2861	2670	N–H... Cl H. bond
1589	1641	1580	1586	1580	N–H ₃ (δ_{as})
1489	1484	1484	1483	1409	N–H ₃ (δ_s)
1404	1399	1400	1402	1409	C–H ₂ (δ_w)(NH ₃) ⁺ sr
1026	1042	1070	1043	1097	ν C–N
870	887	885	885	884	ν C–C
742	717	727	727	730	C–H ₂ (δ_r)
440, 499	414	394, 359	416	544	Torsional C–N

^a This work.

The obtained IR spectrum is typical for alkyl-diammonium perovskites [41]. C–H₂ stretching shows strong bands around 3188 cm^{-1} and 3130 cm^{-1} which have been assigned to the anti-symmetric and symmetric modes respectively. The unique band at 2850–2950 cm^{-1} is expected when hydrogen bonds are formed. The bands at 1588 cm^{-1} and at 1481 cm^{-1} correspond to the asymmetric deformation δ_{as} (NH₃) and symmetric δ_s deformation, respectively. Bands near 1400 cm^{-1} have been assigned to the wagging mode of the CH₂ group. These modes are mixed with the (NH₃)⁺ internal modes. The coupling with the (NH₃)⁺ may be the reason for the strong enhancement of the intensity of the CH₂ wagging modes compared to the corresponding ones in the case of n-alkynes. Bands at 800 cm^{-1} and 700 cm^{-1} are assigned to the CH₂ rocking fundamental mode δ_r (CH₂). Bands below 830 are observed for chains with gauche conformation [13,15,17,34].

3.2. Structure description

The organic–inorganic hybrid perovskite [NH₃(CH₂)₄NH₃]CoCl₄ consists of organic dications [NH₃(CH₂)₄NH₃]²⁺ and inorganic dianions [CoCl₄]²⁻. Fig. 2a and b show an ORTEP view of the molecule and arrangement of molecules in the unit cell. Table 2 lists single crystal data collection and refinement. Table 3 lists selected bond length (Å), bond angles (°) and dihedral angles. The putelenediammonium ion has a zigzag chain structure at N7 side with average C–C bond length of 1.50 Å. The average N–C bond distances are 1.47 Å. These values are in good agreement with bond lengths of other previously studied diammonium salts [42–44]. The anions [CoCl₄]²⁻ form unassociated tetrahedral structure with alternating up and down orientations relative to the c-axis. They are sandwiched between layers of the putelenediammonium chains as shown in Fig. 3a and b. The Co–Cl bond distances are all equal within 0.016 Å with a value of 2.276 Å, the distortions of the bond angles are less than 4 (°) with respect to the perfect tetrahedral. These values are in a good agreement with the previously published data of Co-containing hybrid perovskites [16,17,27–29]. The structure is stabilized by hydrogen bonding between Cl⁻ anion of inorganic layer and the H-atoms of NH₃ at the chain ends of [NH₃(CH₂)₄NH₃]²⁺ cation as well as by the short contacts that are less than the Wan der Waals radii of the atoms. Only three Cl atoms are involved in hydrogen bonding with ammonium groups as shown in Table 4.

The N–H... Cl hydrogen bond strength can be determined by the bond length, the bond N6–H6A–Cl3 and N6–H6B–Cl4 distances are 2.307 Å and 2.324 Å, respectively, which are much stronger than H bonds on N7 side as shown in Table 4. This may be due to the presence of conformation at the N7 side which makes it out of plane of the molecule and the dihydral angle N7–C11–C8–C8 = -68.6 (4) (°), whereas all trans configuration on N6 side has

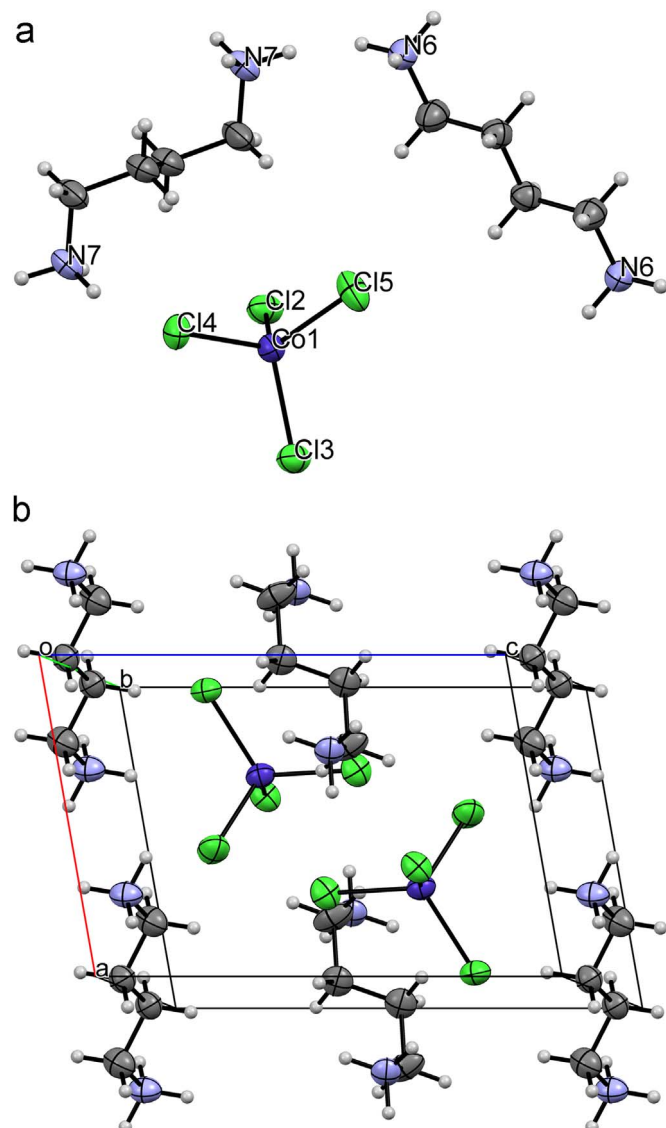


Fig. 2. (a). ORTEP view of the molecule [(NH₃)(CH₂)₄(NH₃)]CoCl₄. (b). Arrangement of molecules [(NH₃)(CH₂)₄(NH₃)]CoCl₄ in the unit cell.

N6–C10–C9–C9 = -180.0 (3) (°). The lamellar structures of [NH₃(CH₂)₄NH₃]CoCl₄ form infinite two dimensional sheets of anions and cations that are parallel to the ac plane as depicted in Fig. 3b. The structure is typically considered as naturally self organized multiple quantum wells with organic layer thickness of

Table 2

Single crystal data collection and refinement of hybrid $[\text{NH}_3(\text{CH}_2)_4\text{NH}_3]\text{CoCl}_4$.

Empirical formula	$\text{C}_4\text{H}_{14}\text{N}_2\text{CoCl}_4$
M_r	290.915
Space group	Triclinic P $\bar{1}$
a	7.2869 (2) Å
b	8.1506 (2) Å
c	10.4127 (3) Å
α	77.2950 (12)°
β	80.0588 (11)°
γ	82.8373 (12)°
V	591.81 (3) Å ³
Z	2
D_x	1.633 Mg m ⁻³
Radiation type	Mo K α
λ	0.71073 Å
θ_{max}	34.99°
μ	2.303 mm ⁻¹
T	298 K
Shape	Prismatic
Color	Blue
Measured reflection	5154
Independent reflections	5154
Observed reflections	2477
Criterion	$I > 2.00 \text{ sigma}(I)$
R_{int}	0.049
H	-11 → 11
K	-12 → 13
L	0 → 16
$R(\text{all})$	0.138
$R(\text{gt})$	0.0646
$wR(\text{ref})$	0.169
$wR(\text{gt})$	0.143
$S(\text{ref})$	0.827
Δ/σ_{max}	0.000
$\Delta\rho_{max}$	0.644 e Å ⁻³
$\Delta\rho_{min}$	-1.7735 e Å ⁻³

Table 3

Selected bond length (Å), bond angles (°) and dihedral angles of $[\text{NH}_3(\text{CH}_2)_4\text{NH}_3]\text{CoCl}_4$.

$[\text{NH}_3(\text{CH}_2)_4\text{NH}_3]\text{CoCl}_4$	
Bond distances (Å)	Co1—Cl5 2.2663 (10) Co1—Cl2 2.2751 (10) Co1—Cl4 2.2799 (9) Co1—Cl3 2.2827 (9)
Bond angels (°)	Cl5—Co1—Cl2 107.46 (4) Cl5—Co1—Cl4 106.90 (4) Cl2—Co1—Cl4 113.73 (4) Cl5—Co1—Cl3 111.82 (4) Cl2—Co1—Cl3 107.73 (4) Cl4—Co1—Cl3 109.25 (4)
Dihedral angle (°)	N7—C11—C8—C8 -68.6 (4) N6—C10—C9—C9 -180.0 (3) C11—C8—C8—C11 180.0 (2) H6A—N6—C10—C9 179.9 H7C—N7—C11—C8 -61.2

6.275 Å and inorganic layer thickness of 3.652 Å. Asymmetric unit consists of one anion together with half of each of two cations on inversion centers. Table 5 lists the crystallographic data of hybrid perovskites of the formula $[\text{NH}_3(\text{CH}_2)_n\text{NH}_3]\text{CoCl}_4$ $n=3, 4, 5, 6, 7, 9$ denoted 2CnCoCl .

It is clearly seen from Table 5 that, as organic chain length increases from $n=3$ up to $n=9$, for the same inorganic layer $[\text{CoCl}_4]^{2-}$, the crystallographic data and crystal symmetry are obviously changed, resulting in lattice parameters and hence unit cell volume increase. Except for $n=3$ [27] and 5 [28] whose unit cell volumes are nearly doubled than other families. This may be

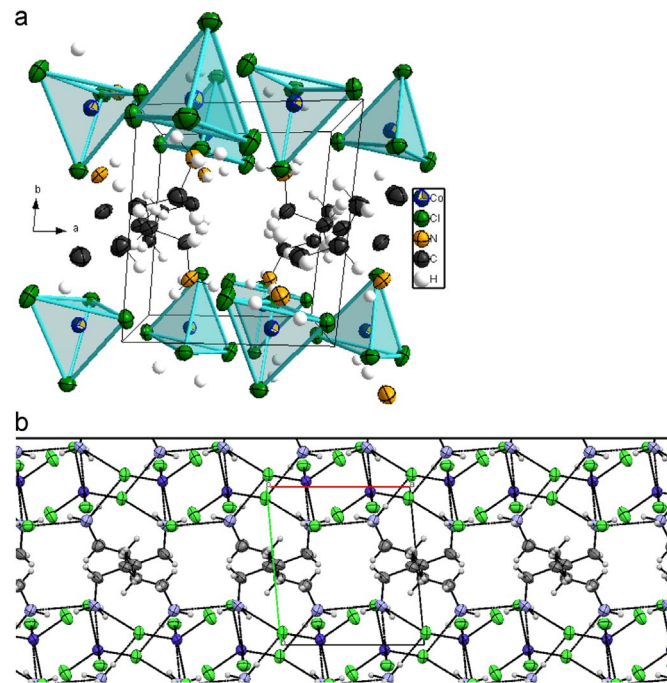


Fig. 3. (a). The polyhedral arrangement of $[\text{CoCl}_4]^{2-}$ along the 001 plan. (b). Lamellar structure and H- bond network parallel to ac plan of the 2D hybrid perovskite $[(\text{NH}_3)(\text{CH}_2)_4(\text{NH}_3)]\text{CoCl}_4$.

Table 4

The H- bond geometry of hybrid $[\text{NH}_3(\text{CH}_2)_4\text{NH}_3]\text{CoCl}_4$.

(D-H-A)	$d(\text{D}-\text{H})$ (Å)	$d(\text{H}-\text{A})$ (Å)	$\angle(\text{D}-\text{H}-\text{A})$ (°)	$D(\text{D}-\text{A})$ (Å)
N6—H6A—Cl3	0.9600	2.307	158.75	3.206
N6—H6B—Cl4	0.9599	2.324	158.98	3.239
N7—H7B—Cl3	0.9600	2.409	145.73	3.248
N7—H7B—Cl2	0.9600	2.910	101.33	3.269
N7—H7C—Cl4	0.9600	2.341	164.65	3.276

related to the crystal symmetry where both $n=3$ and 5 hybrids belong to monoclinic system and all other members are of triclinic system. For $n=6$ and 7 the organic chains acts as spacers between the inorganic layers [16,17,29], similar to the hybrids with $n=4$ and 9 as obtained from this work. But for hybrids with $n=3$ and 5 the organic chains are not sandwiched between inorganic layers. However, the dimensionality (2D) still conserved. Another observation from Table 5 is that the density of the hybrids decreases, while the molecular weight increases regularly by 14 g/mol by adding CH_2 to the molecule from $n=3$ to $n=9$. This is due to the fact that unit cell volume increase is more than the molecular weight increase. The average Co-Cl bond distances for hybrids $n=3-9$ is 2.274 Å varying within 0.007 Å. This indicates that the Co atom is nearly at the center of the tetrahedron. The tetrahedral distortion in Cl-Co-Cl angles is small for all hybrids and varying within 4–5° from the ideal tetrahedral symmetry. So far there are no data available in the literature for $n=8$.

3.3. Lattice potential energy U_{pot} (kJ/mol), lattice enthalpy ΔH_L (kJ/mol), molecular and cation volume V_m , V^+ (nm³) of $[(\text{NH}_3)(\text{CH}_2)_n(\text{NH}_3)]\text{CoCl}_4$, $n=3-9$

Lattice potential energy and lattice enthalpy are essential in determining the stability of new materials, telling us whether new material can be synthesized or not. It is also important to access the thermodynamical parameters involved. An estimation of the lattice potential energy, (U_{pot}) kJ/mol, for a general type of the salts

Table 5

Crystallographic data of hybrids of the formula $[\text{NH}_3(\text{CH}_2)_n\text{NH}_3]\text{CoCl}_4$ $n=3, 4, 5, 6, 7, 9$ denoted 2CnCoCl .

Formula	Mol. wt	<i>a</i> (Å)	<i>b</i> (Å)	<i>c</i> (Å)	α (°)	β (°)	γ (°)	<i>V</i> (Å ³)	sp.gr	ρ Mg m ⁻³	<i>Z</i>	Refs.
2C3CoCl	276.91	10.707	10.647	11.031	90	120	90	1087.6	<i>P</i> 21/c	1.691	4	[27]
2C4CoCl	290.91	7.2869	8.150	10.412	77.295	80.058	82.837	591.81	<i>P</i> 1̄	1.633	2	^a
2C5CoCl	304.93	7.1633	15.940	11.137	90	98.44	90	1257.9	<i>P</i> 21/c	1.610	4	[28]
2C6CoCl	319.05	7.2803	9.9479	9.9572	75.682	87.494	88.790	698.02	<i>P</i> 1̄	1.518	2	[29]
2C7CoCl	332.99	7.3107	10.1841	11.269	66.810	78.858	87.664	756.10	<i>P</i> 1̄	1.463	2	[17]
2C9CoCl	361.05	7.3113	10.2373	12.4701	112.323	92.441	93.452	859.68	<i>P</i> 1̄	1.395	2	#

^a S.K. Abdel-Aal unpublished work CCDC 1437813.

^a This work.

of MpXq by using Eq. (3) according to Ref. [32]:

$$U_{\text{pot}} = \sum_i n_i z_i^2 [\alpha/V_m^{1/3} + \beta] \quad (3)$$

where α and β are appropriate fitted coefficients chosen according to the stoichiometry of the salt, n_i is the number of ions with a charge z_i in the formula unit, V_m is the molecular volume (nm³).

For salts of the type MX (1:1) and MX_2 (1:2), Eq. (3) could be written as:

$$U_{\text{pot}} = |Z^+||Z^-|v [\alpha/V_m^{1/3} + \beta] \quad (4)$$

where Z^+ and Z^- are the respective charges on the cation and anion of the compound, v is the number of ions per molecule and equals to $(p+q)$. In the case of salts of a formula MX with charge ratio (1:1) $Z^+=2$, $Z^-=-2$, $p=1$, $q=1$, $v=2$, $\alpha=117.3 \text{ kJ mol}^{-1} \text{ nm}$, $\beta=51.9 \text{ kJ mol}^{-1}$, and V_m is in units of nm³, the molecular volume (V_m) is given by [33]

$$V_m (\text{nm}^3) = M_m/\rho N_A = 1.66045 \times 10^{-3} M_m/\rho \quad (5)$$

where N_A is Avogadro's number, ρ (g cm⁻³) is the density and M_m (g/mol) is the molar mass as obtained from the crystal structure information listed in Table 1. V_m is calculated from Eq. (5). According to Ref. [34] the anion volume, $[\text{CoCl}_4]^{2-}=0.196 \text{ nm}^3$, thus V^+ (the volume of the cation in $[(\text{NH}_3)(\text{CH}_2)_n(\text{NH}_3)]^{2+}$ ($n=3-9$)) can be easily calculated by subtracting the anion volume from the molecular volume V_m . The lattice enthalpy ΔH_L (kJ/mol) is "enthalpy changes during the process of converting crystalline solid into its constituent gaseous ions", as stated by Mallouk et al. [45]. For the salts MX with the ratio (1:1), there is a linear correlation between ΔH_L (kJ/mol) and inverse cube root of the molecular volume V_m (nm³), as expressed by Eq. (5) using Bartlett's relationship [45]

$$\Delta H_L = \frac{232.8}{\sqrt[3]{V_m}} + 110 \text{ kJ/mol} \quad (6)$$

The lattice potential energy U_{pot} , lattice enthalpy ΔH_L , molecular volume V_m and cation volume V^+ of the $[(\text{NH}_3)(\text{CH}_2)_n(\text{NH}_3)]\text{CoCl}_4$ along with other members of the family $[(\text{NH}_3)(\text{CH}_2)_n(\text{NH}_3)]\text{CoCl}_4$, $n=3, 5, 6, 7$ and 9 are listed in Table 6. Fig. 4.a shows a variation of the lattice potential energy (U_{pot}), cation volume V^+ as a function of number of carbon atoms/chain (n). The solid points represent the data points and the lines represent a linear fit. It is clear that as (n) increases the lattice potential energy decreases linearly for the $[(\text{NH}_3)(\text{CH}_2)_n(\text{NH}_3)]\text{CoCl}_4$ group according to:

$$U_{\text{pot}} = -34.67 n + 1963.1 \quad (7)$$

The cation volume (V^+) increases linearly as a function of the number of carbon atoms/chain (n) according to:

$$V^+(\text{cation}) = 0.026 n - 0.008 \quad (8)$$

Fig. 4b shows the variation of the molecular volume (V_m) and

Table 6

Lattice potential energy (U_{pot}), lattice enthalpy ΔH_L , molecular volume (V_m), cation volume (V^+) and ratio of unit cell volume V/V_m of 2D perovskite hybrid of the formula $[(\text{NH}_3)(\text{CH}_2)_n(\text{NH}_3)]\text{CoCl}_4$, $n=3, 4, 5, 6, 7, 9$.

<i>n</i>	U_{pot} (kJ/mol)	ΔH_L (kJ/mol)	V_m (nm ³)	V^+ (nm ³)	V/V_m	Density (ρ Mg m ⁻³) used in calculation from Refs.
3	1863.12	467.80	0.271	0.075	4.00	[27]
4	1823.01	457.97	0.295	0.099	1.99	^a
5	1794.59	451.01	0.314	0.118	3.999	[28]
6	1747.72	439.53	0.348	0.152	2.000	[29]
7	1712.70	430.94	0.377	0.181	2.000	[17]
9	1658.35	417.62	0.429	0.233	2.000	#

^a S. K. Abdel-Aal unpublished work CCDC 1437813.

^a This work.

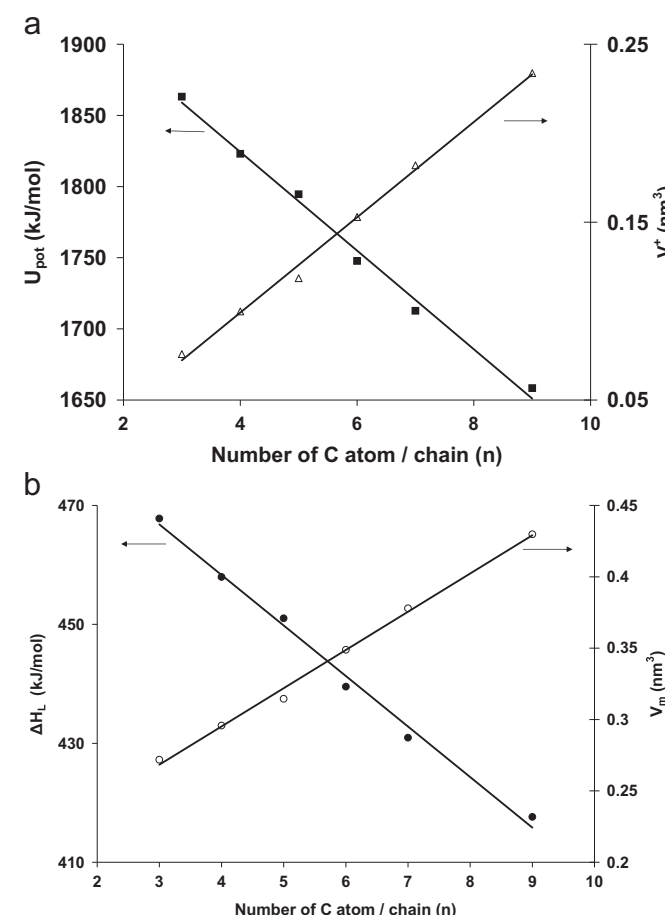


Fig. 4. (a). Variation of lattice potential energy (U_{pot}), cation volume V^+ as a function of number of carbon atoms/chain (n). (b). Variation of lattice enthalpy ΔH_L , molecular volume (V_m) as a function of number of carbon atoms/chain (n).

lattice enthalpy ΔH_L with (n) . Both show linear variation with increasing n according to:

$$V_m = 0.026 n + 0.188 \quad (9)$$

$$\Delta H_L = -8.49 n + 492.3 \quad (10)$$

The ratio, unit cell volume/molecular volume, of the hybrids are also included in **Table 6**, indicating number of molecule per unit cell is in a good agreement with Z from the experimental crystal structure data provided in **Table 5**.

4. Conclusion

We managed to prepare single crystals of the 2D hybrid perovskite of $[(\text{NH}_3)(\text{CH}_2)_4(\text{NH}_3)]\text{CoCl}_4$. The hybrid crystallizes in a triclinic system space group $P\bar{1}$ centrosymmetric, with unit cell parameters $a=7.4042$ (4) Å, $b=10.3484$ (5) Å, $c=11.3554$ (6) Å, $\alpha=66.289$ (3)°, $\beta=78.425$ (2)°, $\gamma=86.546$ (3)°. This is different from the monoclinic system to which short chain diammmonium salts belong. The lattice potential energy U_{pot} and lattice enthalpy ΔH_L are found to decrease as chain length increases. In contrast the molecular volume V_m and cation volume V^+ increase with increasing chain length. The structural properties determined in this work helps us find more organic-inorganic hybrid halide perovskite materials with promising applications involving naturally self assembled multiple quantum well.

Acknowledgment

The authors are grateful to the financial support of Faculty of Science, Cairo University. We thank Dr. Yang Ren from Argonne National Laboratory for discussions.

Appendix A. Supporting information

Supplementary data associated with this article can be found in the online version at <http://dx.doi.org/10.1016/j.jcrysro.2016.08.006>.

All crystallographic data for the structure reported in this paper can be obtained free of charge via Cambridge Crystallographic Data Centre as supplementary publication, deposit number. CCDC. 1401386. Copies of the data can be obtained on application to CCDC, 12 Union Road, Cambridge CB2 1EZ, UK (fax: +44 1223 336 033; e-mail:(deposit@ccdc.cam.ac.uk).

References

- [1] D.B. Mitzi, K. Chondroudis, C.R. Kagan, Organic-inorganic electronics, *IBM J. Res. Dev.* 45 (1) (2001) 29–47.
- [2] Z. Cheng, J. Lin, Layered organic-inorganic hybrid perovskites: structure, optical properties, film preparation, patterning and templating engineering, *Cryst. Eng. Comm.* 12 (2010) 2646–2662.
- [3] S. González-Carrero, R.E. Galian, J. Pérez-Prieto, Organometal halide perovskites: bulk low-dimension materials and nanoparticles, *Part. Part. Syst. Charact.* 32 (7) (2015) 709–720.
- [4] D.B. Mitzi, Synthesis, crystal structure, and optical and thermal properties of $(\text{C}_4\text{H}_9\text{NH}_3)_2\text{MI}_4$ ($\text{M} = \text{Ge}, \text{Sn}, \text{Pb}$), *Chem. Mater.* 8 (3) (1996) 791–800.
- [5] Y. Wei, P. Audebert, L. Galimche, J.-S. Lauret, E. Deleporte, Photostability of 2D organic-inorganic hybrid perovskites, *Materials* 7 (6) (2014) 4789–4802.
- [6] D.B. Mitzi, Templating and structural engineering in organic-inorganic perovskites, *J. Chem. Soc. Dalton Trans.* 1 (2001) 1–12.
- [7] S. Ahmad, C. Hanmandlu, P.K. Kanaujia, G. Vijaya Prakash, Direct deposition strategy for highly ordered inorganic organic Perovskite Thin Films And their optoelectronic applications, *Opt. Mater. Express* 4 (7) (2014) 1313–1323.
- [8] I. Saikumar, S. Ahmad, J.J. Baumberg, G. Vijaya Prakash, Fabrication of excitonic luminescent inorganic-organic hybrid nano- and microcrystals, *Scr. Mater.* 67 (10) (2012) 834–837.
- [9] K. Pradeesh, G.S. Yadav, M. Singh, G. Vijaya Prakash, Synthesis, structure and optical studies of inorganic-organic hybrid semiconductor, $\text{NH}_3(\text{CH}_2)_{12}\text{NH}_3\text{PbI}_4$, *Mater. Chem. Phys.* 124 (1) (2010) 44–47.
- [10] K. Pradeesh, J.J. Baumberg, G. Vijaya Prakash, Exciton switching and Peierls transitions in hybrid Inorganic-organic self-assembled quantum wells, *Appl. Phys. Lett.* 95 (17) (2009) 173305.
- [11] K. Pradeesh, J.J. Baumberg, G. Vijaya Prakash, Strong exciton-photon coupling in inorganic-organic multiple quantum wells embedded low-Q microcavity, *Opt. Express* 17 (24) (2009) 22171–22178.
- [12] S. Kéna-Cohen, M. Davanço, S.R. Forrest, Strong exciton-photon coupling in an organic single crystal microcavity, *Phys. Rev. Lett.* 101 (11) (2008) 116401–116402.
- [13] K. Elmebrouki, S. Tamsamani, J. Aazza, M. Khechoubi, A. Khmou, Synthesis and characterization of new materials like perovskite $[\text{NH}_3-(\text{CH}_2)_n-\text{NH}_3]\text{ZnCl}_4$ avec $n=8$ ET 10, *J. Asian Sci. Res.* 1 (3) (2011) 216–219.
- [14] K. Pradeesh, J.J. Baumberg, G. Vijaya Prakash, In situ intercalation strategies for device-quality hybrid Inorganic-organic self-assembled quantum wells, *Appl. Phys. Lett.* 95 (3) (2009) 033309.
- [15] M.F. Mostafa, A. Hassoun, Phase transition and electric properties of long chain $\text{Cd}(\text{II})$ layered perovskites, *Phase Transit.* 79 (2006) 305–311.
- [16] M.F. Mostafa, S.K. Abdel-Aal, A.K. Tammam, Crystal strucrture, thermal, electric and magnetic study of $[(\text{CH}_2)_7(\text{NH}_3)_2]\text{CoCl}_2\text{Br}_2$, *Indian J. Phys.* 88 (1) (2014) 49–57.
- [17] Mohga Farid Mostafa, Shimaa Said El-khiyami, Seham Kamal Abdel-Aal, Crystal structure, phase transition and conductivity study of two new organic-inorganic hybrids: $[(\text{CH}_2)_7(\text{NH}_3)_2]\text{X}_2$, $\text{X} = \text{Cl}/\text{Br}$, *J. Mol. Struct.* 1127 (2017) 59–73.
- [18] K. Tichy, J. Bene, R. Kind, H. Arend, Second-order phase transition of 1,4-butanediylammonium manganese tetrachloride. A neutron diffraction study on clustered crystals, *Acta Cryst.* B36 (1980) 1355–1367.
- [19] A. Lamhamdi, E. Mejdoubi, K. Fejfarová, M. Dusek, B. EL Bali, Poly[Ethane-1,2-diammonium Tetra-[Mu]-chlorido-cadmate(II)], *Acta Cryst.* E65 (2009) m215–m216.
- [20] C. Courseille, N.B. Chanh, Th Maris, A. Daoud, Y. Abid, M. Laguerre, Crystal structure and phase transition in the perovskite-type layer molecular composite $\text{NH}_3(\text{CH}_2)_4\text{NH}_3\text{PbCl}_4$, *Phys. Stat. Sol. A* 143 (2) (1994) 203–214.
- [21] K. Pradeesh, G.S. Yadav, M. Singh, G. Vijaya Prakash, Synthesis, structure and optical studies of inorganic-organic hybrld Semiconductor, $[\text{NH}_3(\text{CH}_2)_{12}\text{NH}_3]\text{PbI}_4$, *Mater. Chem. Phys.* 124 (2010) 44–47.
- [22] J. Guan, Z. Tang, A.M. Guloy, α - $[\text{NH}_3(\text{CH}_2)_5\text{NH}_3]\text{SnI}_4$: a new layered perovskite structure, *Chem. Commun.* 18 (1999) 1833–1834.
- [23] M. Khechoubi, A. Bendani, N.B. Chanh, C. Courseille, R. Duplessix, M. Couzi, Thermal conformational changes in a bidimensional molecular composite material: a thermodynamic and crystallographic study of $\text{NH}_3-(\text{CH}_2)_4-\text{NH}_3\text{CdCl}_4$, *J. Phys. Chem. Solids* 55 (11) (1994) 1277–1288.
- [24] (-) K. Tichy, J. Bene, W. Hxlg, H. Arend, Neutron Diffraction Study of Twinned Crystals of Ethylenediammonium Copper Tetraehloride and Ethylene-diammonium Manganese Tetrachloride, *Acta Cryst.* B34 (1978) 2970–2981.
- [25] J.K. Garland, K. Emerson, M.R. Pressprich, Structures of four- and five-carbon alkylidiammonium tetrachlorocuprate(II) and tetrabromocuprate(II) salts, *Acta Cryst.* C46 (1990) 1603–1609.
- [26] T. Maris, G. Bravic, N.B. Chanh, J.M. Leger, J.C. Bissey, A. Villesuzanne, R. Zouari, A. Daoud, Structures and thermal behavior in the series of two-dimensional molecular composites $\text{NH}_3-(\text{CH}_2)_4-\text{NH}_3\text{MCl}_4$ related to the nature of the metal M. Part 1: crystal structures and phase transitions in the case $\text{M} = \text{Cu}$ and Pd , *J. Phys. Chem. Solids* 57 (12) (1996) 1963–1975.
- [27] N. Guo, Y.-H. Lin, G.-F. Zeng, S.-Q. Xi, Structure of 1,3-propanediammonium tetrachlorocobaltate(II), *Acta Cryst.* C48 (1992) 542–543.
- [28] J.J. Criado, A. Jiménez-Sánchez, F.H. Cano, R. Sáez-Puche, E. Rodríguez-Fernández, Preparation and characterization of tetrachlorocobaltates(II) of [alpha]-[omega]-alkylenediammonium. Magnetic and thermal properties. Crystal structure of $[\text{NH}_3(\text{CH}_2)_5\text{NH}_3]\text{CoCl}_4$, *Acta Cryst.* B55 (1999) 947–952.
- [29] A.H. Mahmoudkhani, V. Langer, The lamellar architecture of 1,6-hexamethylene-diammonium tetrachlorocobaltate(II), *Acta Cryst.* E58 (2002) 592–594.
- [30] A. Kallel, J. Fail, H. Fuess, A. Daoud, 1,3-Propanediammonium Tetra-chlorozincate(II), *Acta Cryst. B* 36 (1980) 2788–2790.
- [31] K. Elmebrouki, M. Khechoubi, A. Kaiba, A. Belaaraj, D. Mondieigc, P. Negrier, Preparation, crystal structure and caraterization of inorganic-organic hybrid perovskite $[\text{NH}_3-(\text{CH}_2)_{10}-\text{NH}_3]\text{ZnCl}_4$, *J. Asian Sci. Res.* 3 (5) (2013) 454–461.
- [32] H.D.B. Jenkins, H.K. Roobottom, J. Passmore, L. Glasser, Relationships among ionic lattice energies, molecular (formula unit) volumes, and thermochemical radii, *Inorg. Chem.* 38 (1999) 3609–3620.
- [33] H.D.B. Jenkins, L. Glasser, Ionic hydrates, $\text{M}_p\text{X}_q \cdot n\text{H}_2\text{O}$: lattice energy and standard enthalpy of formation estimation, *Inorg. Chem.* 41 (17) (2002) 4378–4388.
- [34] L. Glasser, H.D.B. Jenkins, Internally consistent ion volumes and their application in volume-based thermodynamics, *Inorg. Chem.* 47 (2008) 6195–6202.
- [35] Z. Otwinskiowski, W. Minor, C.W. Carter Jr., Cell refinement: HKL Scalepack, in: R. M. Sweet (Ed.), *Methods in Enzymology*, 276, Publishing Academic Press, NewYork, 1997, pp. 30–326.
- [36] A. Altomare, G. Cascarano, C. Giacovazzo, A. Guagliardi, M.C. Burla, G. Polidori, M. Camalli, SIR92 – a program for automatic solution of crystal structures by direct methods, *J. Appl. Cryst.* 27 (1994) 435–436.
- [37] S. Mackay, C. J. Gilmore, C. Edwards, N. Stewart, K. Shankland, maXus Computer Program for the Solution and Refinement of crystal Structures. Bruker

- Nonius, The Netherlands, MacScience, Japan and The University of Glasgow, 1999.
- [38] R.H. Blessing, An empirical correction for absorption anisotropy, *Acta Cryst. A* 51 (1995) 33–38.
- [39] C.K. Johnson, ORTEP-II. A Fortran Thermal-Ellipsoid Plot Program, Report ORNL-5138, Oak Ridge National Laboratory, Oak Ridge, Tennessee, USA, 1976.
- [40] M.F. Mostafa, A.A.A. Youssef, Magnetic and electric studies of a new Cu(II) perovskite-like material, *Z. Nat.* 59a (2004) 35–46.
- [41] S. Kamoun, A. Daoud, Comparative studies of phase transitions of alkyl chains in $(C_6H_{13}NH_3)_2PbCl_4$, $(C_9H_{19}NH_3)_2PbCl_4$ and $(C_9H_{19}NH_3)_2CdCl_4$, *Phys. Stat. Sol. A* 162 (1997) 575–586.
- [42] C. van Blerk, G.J. Kruger, Butane-1,4-diammonium dibromide, *Acta Cryst. E* 63 (2007) o342–o344.
- [43] C. Arderne, Pentane-1,5-diaminium dibromide, *Acta Cryst. C* 69 (2013) 526–528.
- [44] I. Pospieszna-Markiewicz, W. Radecka-Paryzek, M. Kubicki, Cadaverinium dichloride: a case of centro-non-centrosymmetric ambiguity, *Acta Cryst. C* 62 (2006) o399–o401.
- [45] T.E. Mallouk, G.L. Rosenthal, G. Mueller, R. Brusasco, N. Bartlett, Fluoride ion affinities of germanium tetrafluoride and boron trifluoride from thermodynamic and structural data for $(SF_3)_2GeF_6$, ClO_2GeF_5 , and ClO_2BF_4 , *Inorg. Chem.* 23 (20) (1984) 3167–3173.